Technical Report CoSBi 18/2007

Rate sensitivity analysis of a Beta binders model of lymphocyte recruitment control mechanism

Paola Lecca
The Microsoft Research - University of Trento
Centre for Computational and Systems Biology
lecca@cosbi.eu

Wen Fong Ooi
DISI- University of Trento, Italy
raymondowf@gmail.com

Corrado Priami
The Microsoft Research - University of Trento
Centre for Computational and Systems Biology
DISI - University of Trento
priami@cosbi.eu

Rate sensitivity analysis of a Beta binders model of lymphocyte recruitment control mechanism

Paola Lecca Wen Fong Ooi Corrado Priami

Abstract

The interaction between lymphocyte in the circulation and endothelial cells lining the blood vessels is a crucial control point in the mechanism of chemotactic detection of inflammation sites. This interaction is mediated by a multisptep process, termed lymphocyte recruitment, involving lymphocyte rolling along the endothelium, activation of lymphocyte integrins, adhesion to endothelial ligands and lymphocyte crossing the endothelium. The events of the lymphocyte extravasation, called *diapedesis* is crucial in the pathogenesis of autoimmune neurological diseases, like multiple sclerosis. Recent wet-labs studies provided the data and the observations proving that chemokines modulate the control of the lymphocyte-endothelial cell recognition and regulate the arrest of lymphocyte. In this paper we present a model of lymphocyte recruitment expressed in the formalism of β-binders and we explore its sensitivity in response to changes of the rates of interaction between chemokines and their receptors. The study is motivated by the intention to individuate those ligand/receptor interactions and their kinetic parameters that are significantly influential in determining the firm arrest of the lymphocyte. We focuses the analysis on the rate coefficients of the chemokines interations. By tuning these parameters we estimate the sensitivity of the model to the rapidity of the lymphocyte adhesion, that recent *in vivo* observations suggest to be an important factor determining the final result of the rolling process.

1 Introduction

Lymphocytes roll along the walls of vessels to survey the endothelial surface for chemotactic signals of inflammation, which stimulate the lymphocyte to stop rolling and migrate through the endothelium and its supporting basement membrane. Lymphocyte adhesion to the endothelial wall is mediated by binding between cell surface receptors and complementary ligands expressed by the endothelium.

The attachment (or tethering) of circulating lymphocytes to the vessel wall is labile, permitting lymphocyte to roll in the direction of the blood flow an bringing them into proximity with activating signals, transmitted by chemokines. These cytokines trigger Gi-proteins on tethered lymphocytes to activate a second class of adhesion receptors, integrins, which firmly bind to IgSF members like VCAM-1 and ICAM-1 leading to an arrest of rolling lymphocyte. The arrested lymphocyte uses these integrins interactions to cross the endothelial lining of the blood vessel and migrate into tissue where it can follow subsequent chemoattractive gradients. This paradigm has been validated for mature blood cells both *in vivo* and *in vitro* [2, 17]. Few years ago a novel intravital microscopy model was developed to directly analyze through the skull the interactions between lymphocytes and the endothelium in cerebral venules of mice [17]. The phenomenology of lymphocyte recruitment on the inflamed endothelium is attracting the attention of scientific community because its crucial role in inflammatory autoimmune diseases like multiple sclerosis. Understanding the molecular basis of the dynamics, and most importantly the sensitivity of the model to the those kinetic parameters governing the rapidity of the lymphocyte adhesion and modulating the frequency of firm arrest cases.

The recent advancements in technology and the increasing maturity in experimental methods are disclosing the molecular mechanisms of the lymphocyte recruitment on the inflammation sites and allow accurate measurements of the hemodynamic and kinetic parameters related to the rolling of the lymphocyte along the endothelium [1, 8, 11, 12, 15, 20, 21]. In turn, the increasing availability of accurate data enables the modelling and the simulation of the recruitment process *in silico*, on a computer. In this paper we present a novel model of lymphocyte recruitment specified in the Beta binders formalism [6, 18] and an analysis of the sensitivity of the model response to changes of the rate coefficients of the interaction between the chemokines expressed on the endothelium and their receptors on the lymphocyte. Our study focuses the sensitivity analysis on such parameters because the chemokines activation stirs up the activation of those integrins responsible for the firm arrest of the cell and its migration into the tissue, principal cause of autoimmune diseases. This work is inspired by a previous study of Lecca et al. [5, 14], in which a model of lymphocyte recruitment specified in biochemical stochastic π-calculus was developed and simulated using the

experimental data obtained from intravital microscopy experiments by Constantin et al. [17]. Therefore, the present study has to be intented also as a demonstration of the greater flexibility and adequacy of the Beta binders language w. r. t. π-calculus in describing parallel highly specific molecular interactions.

2 Mechanism of Lymphocyte recruitment

A critical event in the pathogenesis of multiple sclerosis, an autoimmune disease of the central nervous system, is the migration of lymphocytes (from brain vessels to brain parenchima). The extravasation of lymphocytes is mediated by highly specialized groups of cell adhesion molecules and activation factors. The process leading to lymphocytes migration is divided into four main kinetic phases: 1) initial contact with the endothelial membrane (tethering) and rolling along the vessel wall; 2) activation of a G-protein, induced by a chemokine exposed by the inflamed endothelium and subsequent activation of integrins; 3) firm arrest; 4) crossing of the endothelium (diapedesis). We rely here on a model of early inflammation in which brain venules express E- and P-selectin, ICAM-1 and VCAM-1 [17]. The leukocyte is represented by encephalitogenic $CD4^+$ T lymphocytes specific for PLP139-151, cells that can induce experimental autoimmune encephalomyelitis (the animal model of multiple sclerosis).

The tethering and rolling steps are mediated by binding between cell surface receptors and complementary ligands expressed on the surface of the endothelium. The principal adhesion molecules involved in these phases are the selectins: the P-selectin glyco-protein ligand-1 (PSGL-1) on the autoreactive lymphocytes and the E- and P-selectin on the endothelial cells. The action of integrins is partially overlapped to the action of selectins/mucins: α_4 integrins and LFA-1 are also involved in the rolling phase, but with a less relevant role.

Chemokines have been shown to trigger rapid integrin-dependent lymphocyte adhesion *in vivo* through a receptor coupled with G_i proteins. Integrin-dependent firm arrest in brain microcirculation is blocked by pertussis toxin (PTX), a molecule able to ADP ribosylate G_i proteins and block their function. Thus, as previously shown in studies on naive lymphocytes homing to Peyer's patches and lymphonodes, encephalitogenic lymphocytes also require an in situ activation by an adhesion-triggering agonist which exerts its effect via Gi-coupled surface receptor.

The firm adhesion/arrest is mediated by lymphocyte integrins and their ligands from the immunoglobulin superfamily expressed by the endothelium. The main adhesion molecules involved in cell arrest is integrin LFA-1 on lymphocyte and its receptor ICAM-1 on the endothelium. The action of α_4 integrins is partially overlapped to the action of LFA-1: α_4 integrins are

involved in the arrest but they have a less relevant role [17].

3 The Beta binders formalism

Beta binders (β-binders) [6] is a formal language that merges the basic features of classical π-calculus [16] with the intuition that, in order to better represent the concepts of specific interaction sites of a biological entity, the π-calculus concurrent processes can be wrapped by borders equipped with explicit interaction sites.

A process in β-binders, termed *bio-process*, is defined as a box with a proper border and an internal machinery. The entities lying within the borders, termed π-*processes*, are formally made up of a certain number of operators that allow to express the possible ways of evolution of the bio-process. In a pictorial view the enclosing borders resemble the interface that the biological entity exhibits to the external view. This interface is pare metrically defined by a set of *binders* (called *beta binders*), representing and specifically characterising the interaction sites (see Fig. 1). We refer the reader to [6] for an introductory reading about the original formulation of β-binders language. Here we report the basics of BetaSim language, giving the formal definition of bio-process and π-process.

The BetaSIM language [7, 19] is based on the stochastic extension of β-binders [18], where the time evolution of the system of bio-processes is driven by the values of stochastic rates, representing the specific speed of interaction between bio-processes and between the processes inside the box. These rates abstract the rates coefficients of the chemical reactions defined in the stochastic formulation of chemical kinetics [10]. Like in the π-calculus, also in the β-binders the biological entities are represented as computational processes an the chemical interactions as pairwise communications between the processes on shared channels. With respect to the original syntax, in BetaSIM several modifications have been introduced. All the modifications are deeply discussed in [7, 19]. A BetaSIM program, called also β-system, is a tuple $Z{=}\langle B, E, \xi\rangle$ which is a composition of a bio-process B, a list of *events* E and *ambient* ξ. The bio-process B intuitively represents the structure of the system, that is a set of entities interacting in the same environment, E represents the list of possible events enabled on the system and the ambient ξ contains information about the environment, that, for clearness reasons, we will discuss in more detail later. The bio-process B, the list of events E, and the binders are defined according to the grammar reported in Table 1.

Processes P are referred as π-*processes*. A π-process P can be a deadlock process (*nil*), i. e. a process that can do nothing, a parallel composition of π-processes, $P|P$, an *action*-prefixed process $\pi.P$, a replicated π-process, $!\pi.P = \pi.P|!\pi.P$, and a non-deterministic choice $M + M$, where M is a π-process in turn. π denotes an *action*. Besides the standard actions of the π-

calculus, as receiving a name y on a channel x ($x(y)$), sending a name y on a channel x ($\overline{x}\langle y\rangle$), and the silent action τ, π-processes exhibit new interaction capabilities, i. e. *change* (*ch*), *die*, *expose*, *hide*, and *unhide*, employed to describe the evolution of the bio-process interface. As we will see later, they represent monomolecular reactions. Boxes are defined as π-processes prefixed by specialised binders that represent interaction capabilities. An *elementary beta binder* has the form $\beta(x, r, \Gamma)$ (active), $\beta^h(x, r, \Gamma)$ (hidden) or $\beta^c(x, r, \Gamma)$ (complexed), where the name x is the subject of the beta binder and Γ represents the type of x.

P	::=	$\mathsf{nil} \mid P\vert P \mid !\pi.P \mid M$
M	::=	$\pi.P \mid M + M$
π	::=	$x(y) \mid \overline{x}\langle y\rangle \mid (\tau, r) \mid (\mathsf{ch}(x, \Delta), r) \mid$
		$(\mathsf{die}, r) \mid (\mathsf{hide}(x), r) \mid (\mathsf{unhide}(x), r) \mid$
		$(\mathsf{expose}(x, s, \Delta), r)$
$\widehat{\beta}$	::=	$\beta \mid \beta^h \mid \beta^c$
$\vec{B}$	::=	$\widehat{\beta}(x, r, \Delta) \mid \widehat{\beta}(x, r, \Delta)\vec{B}$
B	::=	$\mathsf{Nil} \mid \vec{B}[P] \mid B\vert\vert B$
cond	::=	$\vec{B}[P] : r \mid \vert\vec{B}[P]\vert = n \mid$
		$\vec{B}[P], \vec{B}[P] : r$
verb	::=	$\mathsf{new}(n) \mid \mathsf{split}(\vec{B}[P], \vec{B}[P])$
		$\mathsf{join}(\vec{B}[P]) \mid \mathsf{delete}$
event	::=	$\mathsf{when}\ (cond)\ verb$
E	::=	$\bullet \mid event \mid event :: E$

Table 1: BetaSIM language syntax.

A bio-process B is either a deadlock bio-process *Nil* or a parallel composition of boxes $\vec{B}[P]$. Let refer to the Fig. 1. The pairs $x_i : \Delta_i$ represent the sites through which the box may interact with other boxes. *Types* Δ_i express the interaction capabilities at x_i. The value r represents the stochastic rate associated to the name x inside the box, h represents the hidden status and the vertical dash over the last beta binder represents the *complexed* status.

Finally, the information contained in the environment ξ consists in the set T of the considered *types* (ranged over by Δ, Γ_0, Σ', $\cdots$), a function $\rho : \mathcal{N} \to \mathbb{R}$ that associates stochastic rates to the action names in $\mathcal{N}$ and the function $\alpha : T^2 \to \mathbb{R}^3$, which describes the affinity relation between couples of types. In particular, given two types Δ and Γ, the application of $\alpha(\Delta, \Gamma)$ returns a triple of stochastic rates (r, s, t), where r, denoted with $\alpha_c(\Delta, \Gamma)$, represents the *complexation rate*, s, denoted with $\alpha_d(\Delta, \Gamma)$, represents *decomplexation rate* and t, denoted with $\alpha_i(\Delta, \Gamma)$, represents the

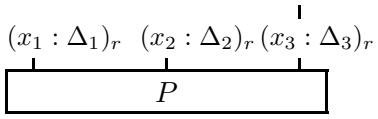

Figure 1: Graphical representation of a bio-process $\vec{B}[P]$ exposing three binders $(x_1 : \Delta_1)_r$, $(x_1 : \Delta_1)_r$, and $(x_3 : \Delta_3)_r$, and containing a π-process P. See in the text for the formal definition of π-processes and bio-processes.

inter-communication rate. The rates can assume also an infinite value (*inf*) to indicate that the communication is instantaneous.

The evolution of the system is formally specified through the *operational semantics* of the language, which defines the actions of *intra communication* involving the π-processing inside a box, *inter communication* between two boxes, *join operation*, specifying the merging of to boxes and *split operation* defining the splitting of a box into two boxes. These operations/actions can be used to express mono-molecular and bi-molecular biochemical reactions.

Mono-molecular actions describe the evolution of single boxes. More precisely, an *intra communication* action allows components to interact within the same box, the *expose* action adds a new site of interaction to the interface of the box containing the expose, the *change* action modifies the type of an interaction site, *hide* and *unhide* actions make respectively invisible and visible an interaction site. Finally, the *die* action eliminates the box. The *complex* operation creates a dedicated communication binding between boxes over compatible - i. e. binders whose types have non null intersection - and unhide elementary beta binders, while the *decomplex* operation destroys an already existing dedicated. A linkage that connects the two interfaces illustrates the formation of complex between two binders whose types are such that $\Delta \cup \Gamma \neq \emptyset$ (Fig. 2).

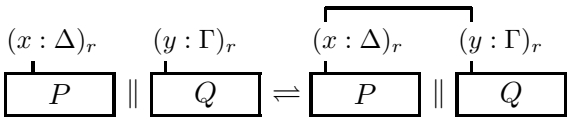

Figure 2: The *complex* operation creates a dedicated communication bond, whereas a *decomplex* operation destroy it.

The stochastic rates associated to complex and decomplex operations are $\alpha_c(\Delta, \Gamma)$ and $\alpha_d(\Delta, \Gamma)$, respectively. The information about the existing dedicated bindings is maintained in the ambient.

The *inter-communication* is also bi-molecular action that can be used to abstract bi-molecular reactions. It enables interaction between boxes

over compatible and unhide elementary beta binders. Let the types associated to the involved elementary beta binders be represented by Δ and Γ . If $\alpha_c(\Delta, \Gamma) > 0$, then the *inter-communication* is enabled, with rate $\alpha_i(\Delta, \Gamma)$, only after a dedicated communication binding, over the involved beta binders, has been created by a *complex* operation. Otherwise, the *inter-communication* is simply enabled with rate $\alpha_i(\Delta, \Gamma)$.

Events can be considered as an implementation of the rules describing the way in which tow boxes can join together and those for the splitting of a box into two boxes, namely, an event is the composition of a condition *cond* and an action *verb*, which is triggered only if the event condition is fulfilled on the structure of the bio-process representing the system. The operations of *join* and *split* can be used to render biological endocytosis, namely the absorption of substances from the external environment. Finally, the event *new* denotes the creation of new boxes ($new(n)$ denotes the generation - also chemical synthesis - of n copies of a box), whereas the event *delete* eliminates a box from the system, and can be used to represent the chemical degradation.

4 The β-binders specification of lymphocyte recruitment

Lymphocytes and ligands on the activated brain endothelial cells are modeled as bio-processes. The molecules P-Selectin, ICAM-1, VCAM-1, and CHEMOKINE, that are expressed on the endothelium, are represented by bio-processes as in Fig. 3. The lymphocyte is represented by the bio-process depicted in Fig. 4. The interface of the bio-process LYMPHOCYTE presents four binders, representing the interaction sites specific for the corresponding four endothelial molecules.

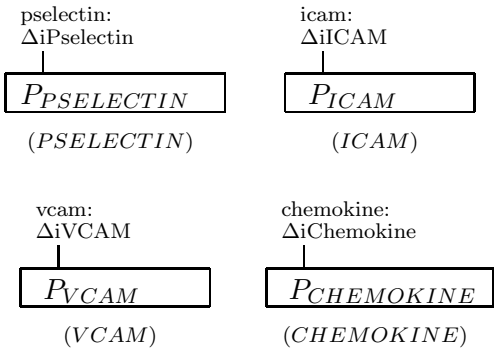

Figure 3: Graphical representations of adhesion molecules.

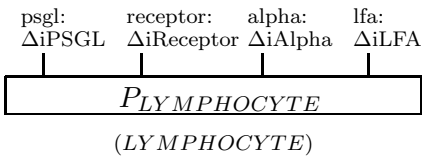

Figure 4: Graphical representation of lymphocyte. It is inspired to the real biological structure depicted in Fig. 16 in Appendix B.

The π-processes are defined as in the following:

$$P_{SELECTIN} := !r.\overline{pselectin}.\overline{r}.\mathsf{nil} | \overline{pselectin}.\overline{r}.\mathsf{nil} \quad (1)$$

$$P_{VCAM} := \mathsf{nil}, \quad P_{ICAM} := \mathsf{nil} \quad (2)$$

$$P_{CHEMOKINE} := !r.\overline{chemokine}.\overline{r}.\mathsf{nil} | \overline{chemokine}.\overline{r}.\mathsf{nil} \quad (3)$$

$$P_{LYMPHOCYTE} := psgl.\mathsf{ch}(psgl, iPSGL2).receptor.\mathsf{unhide}(alpha).\mathsf{unhide}(lfa).\mathsf{nil} \quad (4)$$

The formation of a tethering bond between the lymphocyte and the endothelium is modeled by a *complex* operation involving the binders ($psgl1 : \Delta iPSGL$) and ($pselecting : \Delta iPselectin$), defined on the interfaces of the bio-processes LYMPHOCYTE and PSELECTIN, respectively (see Fig. 5).

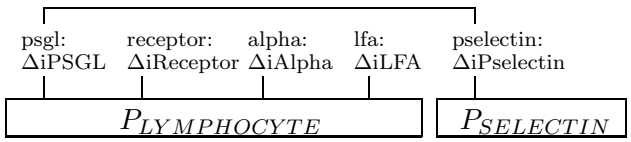

Figure 5: The formation of $LYMPHOCYTE\_PSELECTIN$ through *complex* operation and $\alpha(\Delta$ iPSGL,Δ iPselectin$)=(m, n, inf)$, and $m, n > 0$.

Once the complex operation has done, inter communication between these two bio-processes takes place instantaneously, i. e. at infinite rate. $P_{SELECTIN}$ acts as a sender and $P_{LYMPHOCYTE}$ acts as a receiver (see formulas (2) and (4)). A message is sent through and received by respective channel. The change of ΔiPSGL to ΔiPSGL2 occurs upon receiving the message which in turn indicates the lymphocyte enters rolling state. The structure is indicated as $LYMPHOCYTE_{ROLL}$, as in Fig. 6 where

$$P_{LYMPHOCYTE\_ROLL} := receptor.unhide(alpha).unhide(lfa).nil \quad (5)$$

The bond between LYMPHOCYTE and PSELECTIN can be broken at dissociation rate, C_d which is defined in the second parameter of α function. After breaking apart, $LYMPHOCYTE_{ROLL}$ and $PSELECTIN$ are restored.

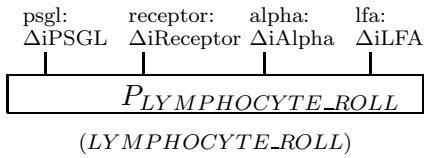

Figure 6: Graphical representation of lymphocytes in rolling state.

The binding of the chemokines to their recptors activates the integrins. It is represented by an inter communication through the binders ΔiChemokine and ΔiReceptor on $CHEMOKINE$ and $LYMPHOCYTE$ respectively. Inter communication between $CHEMOKINE$ and $LYMPHOCYTE_{ROLL}$ takes place immediately after complexation by sending a dummy message to trigger the activation. The bio-process $CHEMOKINE$ is the sender while $thebio - processLYMPHOCYTE_{ROLL}$ is the receiver. Upon receiving the message from $CHEMOKINE$, the hidden interfaces, ΔiAlpha and ΔiLFA are unhidden. Such an abstraction represents successful activation of integrins. After the activation, ΔiLFA and ΔiAlpha are unhidden. The unhidden interfaces prepares $LYMPHOCYTE\_ROLL$ to be arrested on the endothelial cells. The interaction between LFA-1, α_4-integrins with ICAM-1 and VCAM-1 respectively in an exact recruitment system is represented by the complex formation and breakage through ΔiLFA, ΔiICAM and ΔiAlpha, ΔiVCAM.

The model is simulated under the setting of amounts of ligands and lymphocytes, spatial parameters and kinetics as in [14]. The length of the brain vessel is $100\mu m$, its radius is $25\mu m$ so that the mechanism is simulated in a space of volume of $1.96 \times 10^5 \mu m^3$. Initial quantity of $LYMPHOCYTE$, $PSELECTIN$, $ICAM$, $VCAM$ and $CHEMOKINE$ are 88, 88, 86, 15, and 236 respectively in the simulation system. The stochastic engine driving the evolution of the system of bio-processes is the Gillespie algorithm [10]. Stochastic rates of association and dissociation, respectively C_a and C_d, and for the interactions governing the four phases of the recruitment, are derived from the deterministic rates k_{on} and k_{off} reported in [13, 14] (and here in Table 2), through the formulas $C_a = 2k_{on}/V$ and $C_d = k_{off}/V$. In our simulation all rates are amplified by 10^4 with assumption that the number of molecules in the preset volume of brain microvessel is the order of 10^4. Moreover, unless it is explicitly stated, all the rate values are measured in s^{-1}.

Process	$k_{on}(s^{-1})$	$k_{off}(s^{-1})$	Reference
Tethering	84	1	[3]
Rolling	84	100	[3]
Activation of Chemokines	0.5	75	[13]
Firm Adhesion	84	20	[3]

Table 2: Deterministic rates for the 4-phases of lymphocyte recruitment.

5 Simulation results

The simulation of the model has been performed for three configurations: (i) with all the rate coefficients at the orginal values, (ii) with all the rates decreased by 10, and (iii) with all the rates decreased by 100. The number of bonds between the ligands and the corresponding receptors of each molecular interactions are shown in Fig. 8. Let focus the analysis to the red curves. In PSGL-1/P-Selectin binding (Fig. 8(A)), the slope is steep at the beginning. After 0.02 seconds, the number of bonds steadily fluctuates within 80 and 88. On the other hand, the activation process (the binding of chemokine to its receptor) is in slower pace at the beginning (Fig. 8(B)). The number of bonds is stable after 0.15 seconds but the amount of bounded molecules varies more significantly within a short time frame. The approximate difference can be as low as 52 bonds and as high as 68 bonds. The results of simulation (Fig.7) are in agreement with those obtained from the π-calculus model in [14] and describe the phases of the mechanism of lymphocyte recruitment. The pre-requisite of integrins' activation (LFA-1,α_4) is the tethering and rolling process. Fig.7 (A) successfully demonstrates the rising of PSGL-1/P-selectin binding is followed by a gradual increase in receptor/chemokine binding. The decreasing volume in tethering (Fig.7 (B)) portrays the state-shift in lymphocytes from free-flowing to rolling.

The response of LFA-1 and α_4 towards the ligands after the activation by chemokines is depicted in Fig. 8 (C). The binding of LFA-1/ICAM-1 is almost immediate and parallel to the activation at the initial simulation time. α_4 binding to its corresponding ligand, VCAM-1, is slightly late in comparison with the immediate response of LFA-1 (Fig.8 (D)). It is worth noting that the number of LFA-1/ICAM-1 is restricted by the number of receptor/chemokine. However, this phenomenon lasts a short time after the beginning of tethering. LFA-1/ICAM-1 amount overtakes receptor/chemokine at about 0.033 seconds. This is due to the fact that receptor/chemokine dissociates at a faster rate and the free chemokines promptly attach to other lymphocytes. The number of α_4/VCAM-1 bonds, after 0.1 s, becomes constant, because the number of α_4 far exceeds the number of available VCAM-1 ligand on the endothelial cells. The ratio is 88:15.

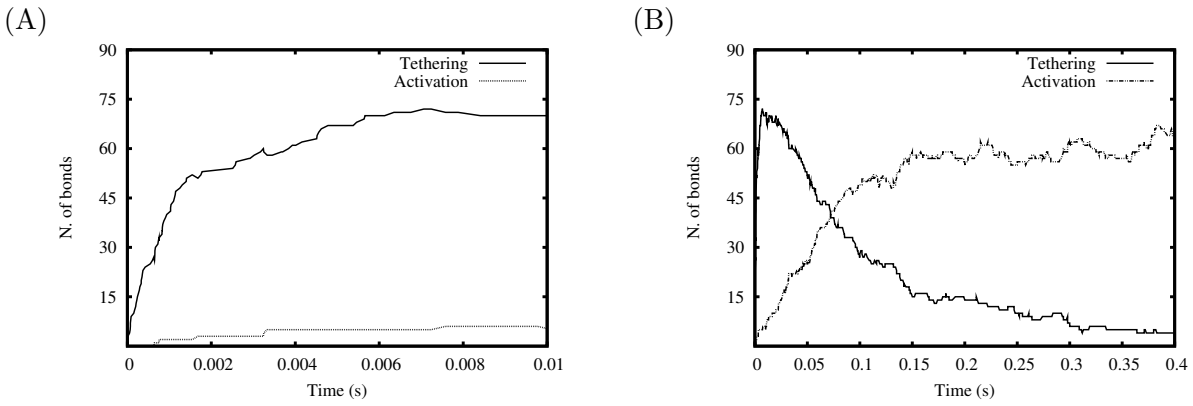

Figure 7: The binding of chemokine ligand-receptors (dotted line) occurs after tethering (solid line).

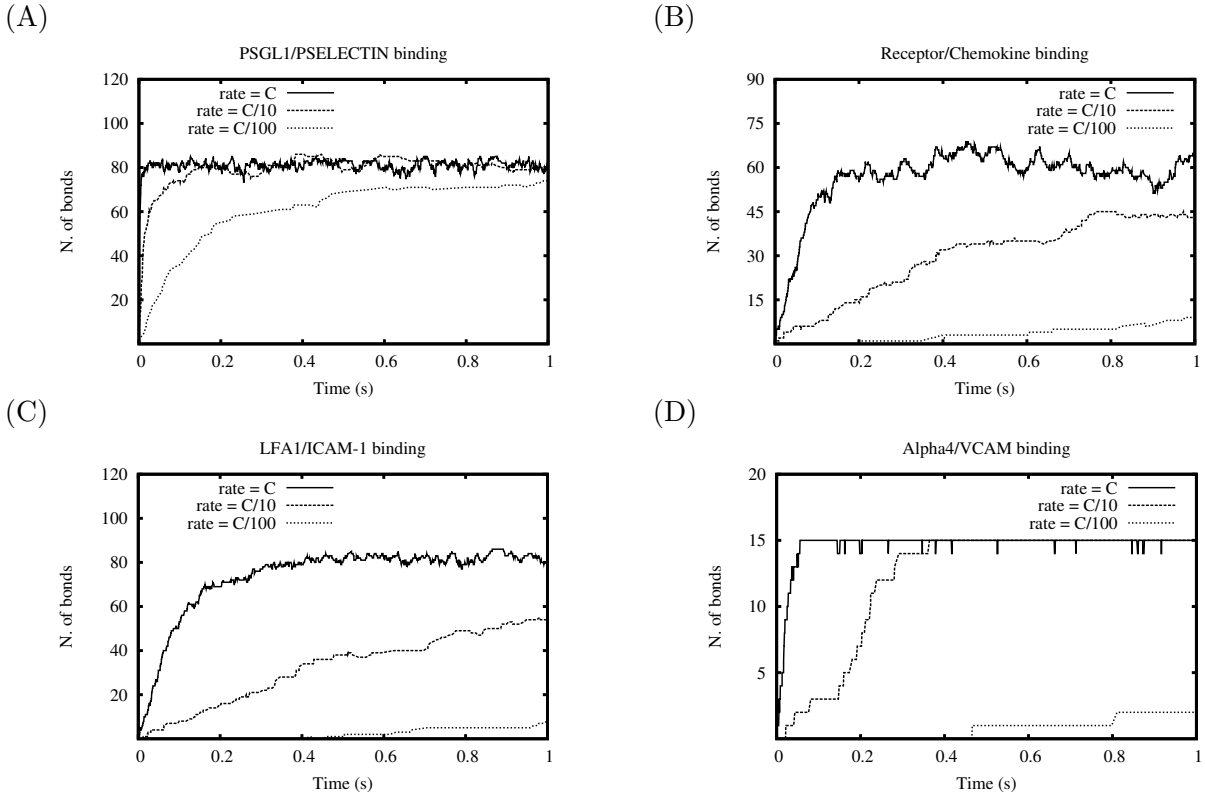

Figure 8: Simulations with all rates at original setting (solid line), with all rates decreased by 10 (dashed lines), and with all rates decreased by 10^2 (dotted line)

In the next section, we will look into the sensitivity of the model in-

cluding overall sensentivity based on different decrement rates; model's responsiveness to the change of VCAM-1's total amount; effect of different association/dissociation rates of receptor/chemokines binding and the casual consequence of activated LFA-1 on lymphocytes to the attachment to ICAM-1.

5.1 Sensitivity analysis

Three major sensitivity analyses were conducted. Let C_a and C_d denote respectively stochastic association and dissociation rates of the interactions between chemokines and their receptors.

5.1.1 Analysis with decreasing rate coefficients.

The time behavior of number of bonds for each molecular interactions in three simulations (Fig.8.) exhibits significant differences. Decreasing the rates results in a less frequent process of binding/unbinding between the ligands and their receptors. Since the chemokine-receptors system triggers the integrin-dependent firm arrest of lymphocytes, an insufficient number of interactions between chemokines and chemokines receptors, even in a situation of lymphocyte rolling with low speed, could cause a firm arrest of the cell out of the area relevelant to the adhesion-triggering stimulus.

5.1.2 Analysis with different amounts of VCAM-1.

The simulations with 15 instances of VCAM-1 (Fig. 9: solid line), 88 VCAM-1 (Fig.9: dotted line) and 176 VCAM-1 (Fig. 9: dashed line) were run. The results in Fig. 9 show that VCAM-1, in presence of excessive amounts of α_4, are rapidly saturated so that the rate of variation of the number of α_4/VCAM-1 bonds rapidly zeroes. VCAM-1 in excessive amount and equivalent amount of lymphocytes (dashed and dotted curves in Fig. 9) show different behavior on the graph w. r. t. the case in which both or them are present in small quantities.

However the velocity of the binding reaction between α_4 and VCAM-1 within the very first instants of the simulation is the same in all the three cases.

5.1.3 Analysis with different C_a, C_d

Simulations were run under different C_a and C_d of receptors to chemokines. The objective of the analysis is to identify the relationship between different combinations of C_a, C_d and the subsequent effect on the time behavior of the

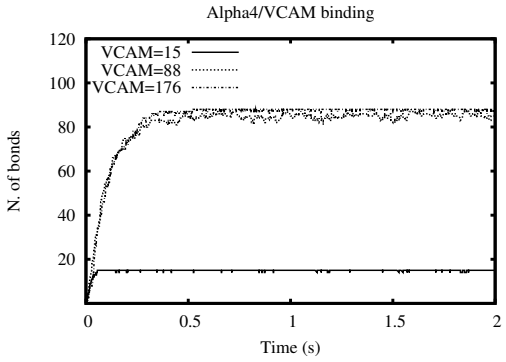

Figure 9: The α_4/VCAM-1 binding with the total VCAM-1 of 15, 88, 176 in corresponding to red, green and blue curves.

number of bonds between chemokines and their receptors and LFA-1 and ICAM-1 molecules. The modified rates are twice higher and lower than the original rate. The analysis is divided into six categories as in the following.

5.1.3.1 Original C_a and changing C_d (Fig.10)

Given the solid line in Fig. 10 as reference, we realize that decrement of C_d yields more receptor/chemokine bonds than increment of C_d. However, the number of lymphocytes (LFA-1) attaching to ICAM-1 in Fig. 10 ((B), dashed line) and Fig. 10((B), dotted line) is almost the same. The lower amount of receptor/chemokine bonds in Fig10 ((A), dotted line) does not indicate that the number of activated LFA-1 is less. This is due to the detachment of the chemokine from its receptor and the formation of another bond later. Thus, the number of receptor/chemokine bonds (Fig. 10 (A), dotted line) is lower. However, it does not results in a consequent difference in the amount of in LFA-1/ICAM-1 complexes, as we expected.

5.1.3.2 Increased C_a and changing C_d (Fig.11)

Increment of C_a does not contribute to a increase the number of LFA-1/ICAM-1 complexes. Both the decreased and the increased C_d (with respect to the original value 3.82) produce almost the same amount of LFA-1/ICAM-1 bonds, whose time-behavior curve slightly lies below the curve of original setting (Fig. 11 (B): solid line). For a fixed value of C_a a decreased C_d is only responsible for a longer time of LFA-1 attachment to ICAM-1; an increased C_d means a faster dissociation of the chemokine from its receptor, but if C_a does not change, variations of C_d seem to not affect the number of bonds between LFA1 and ICAM1.

(A) (B)

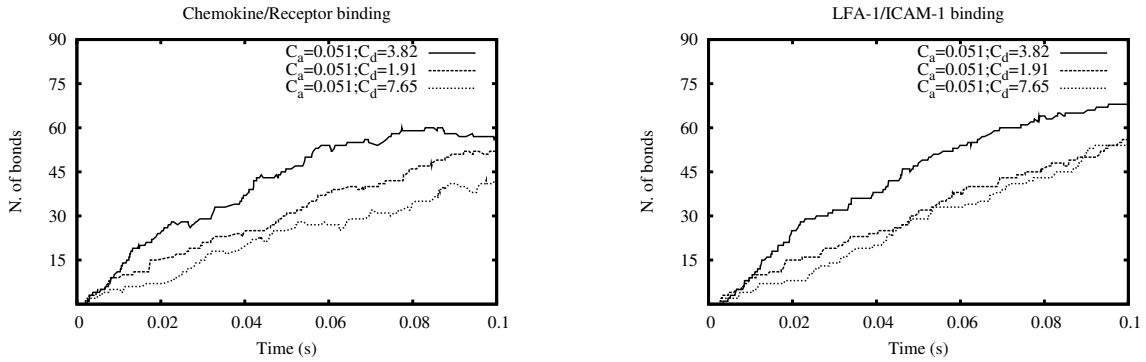

Figure 10: (A) The number of bonds between chemokines and their receptors at $C_a = 0.051$ and $C_d = 3.82,\ 1.91,\ 7.65$; (B) The time behavior of the number of LFA-1/ICAM-1 bonds, consequent on the activation of chemokine's receptors.

(A) (B)

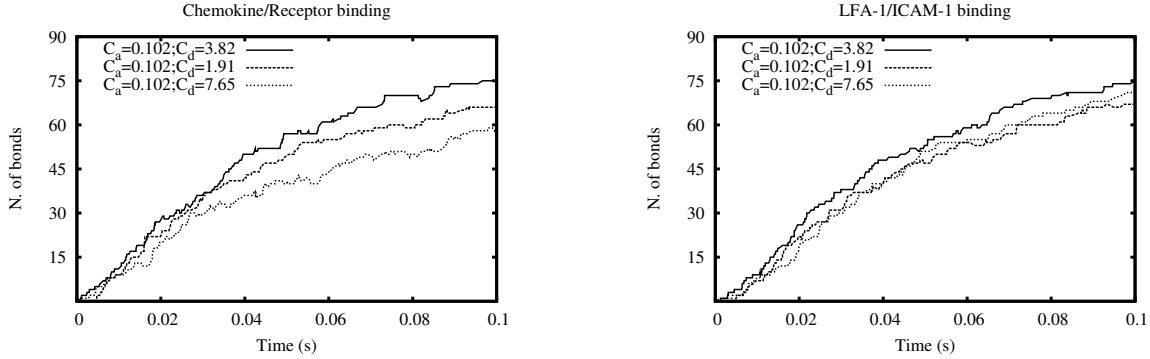

Figure 11: (A) The number of bonds between chemokines and their receptors at $C_a = 0.102$ but at $C_d = 3.82, 1.91, 7.65$; (B) The time behavior of the number of LFA-1/ICAM-1 bonds consequent on the activation of chemokine's receptors.

5.1.3.3 **Decreased C_a and changing C_d (Fig.12)**

The model does not respond sensitively to these configurations. The number of bound elements grows in insignificantly difference.

(A) (B)

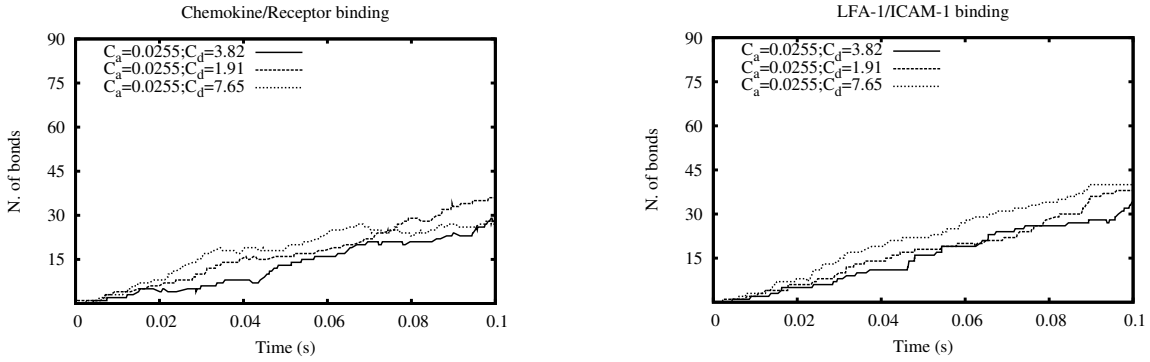

Figure 12: (A) The number of bonds between chemokines and their receptors at $C_a = 0.0255$ but at $C_d = 3.82, 1.91, 7.65$. (B) The LFA-1/ICAM-1 bindings that depends on the activation of chemokine's receptors.

(A) (B)

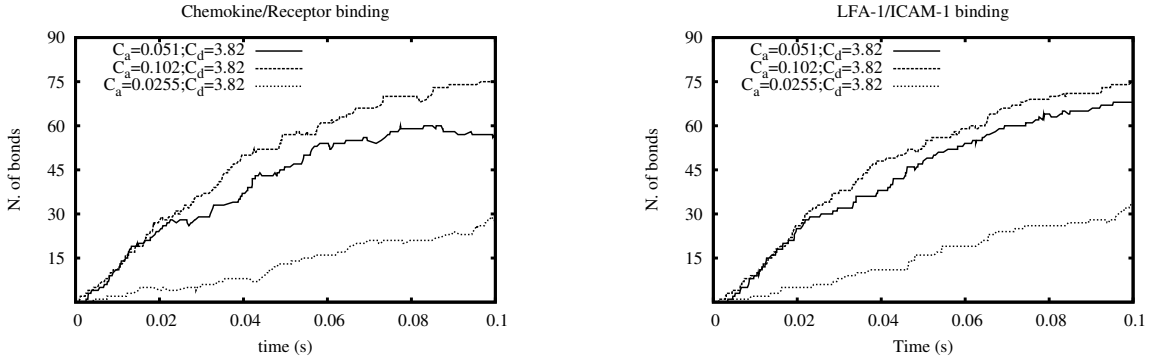

Figure 13: (A) The number of bonds between chemokines and their receptors at $C_d = 3.82$ but at $C_a = 0.051, 0.102, 0.0255$. (B) The LFA-1/ICAM-1 number of bonds consequent on chemokines receptors activation.

5.1.3.4 **Original C_d and changing C_a (Fig.13)**

The decrement of C_a shows significant difference in the number of bonds over the time (Fig.13 ((A), dashed line). In this case, a low value of C_a causes a proportionally low number of activated LFA-1. A double value of C_a causes higher number of bonds of activated LFA-1 after 0.02 s (Fig.13 ((A), solid line)).

5.1.3.5 **Decreased C_d and changing C_a (Fig.14)**

At a low C_d, the model is sensitive to the change in C_a. This is apparent in the binding of receptor/chemokine and LFA-1/ICAM-1. The high propensity of the chemokine to form a complex with its receptors (Fig.14((A), dashed line) could have induced more activated

LFA-1 of lymphocytes which consequently produces higher numbers of LFA-1/VCAM-1 bonds.

(A) (B)

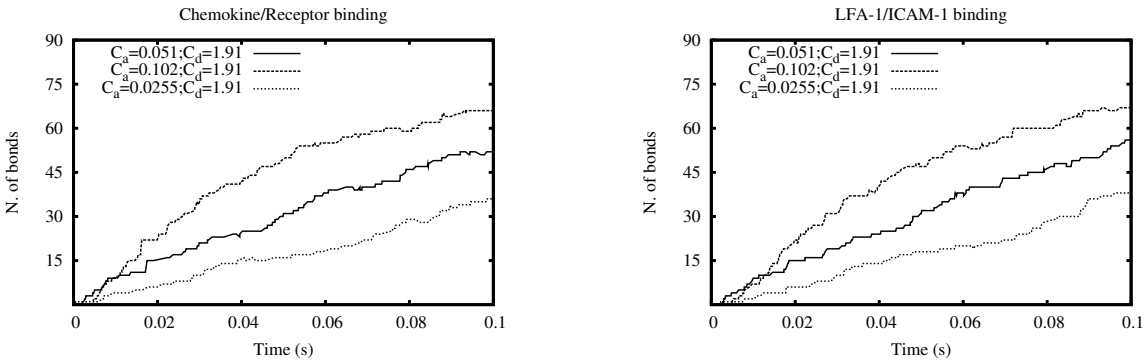

Figure 14: (A) The number of bonds between chemokines and their receptors at $C_d = 1.91$ but at $C_a = 0.051, 0.102, 0.0255$. (B) The LFA-1/ICAM-1 number of bonds consequent on chemokine's receptors activation.

5.1.3.6 **Increased C_d and changing C_a (Fig.15)**

(A) (B)

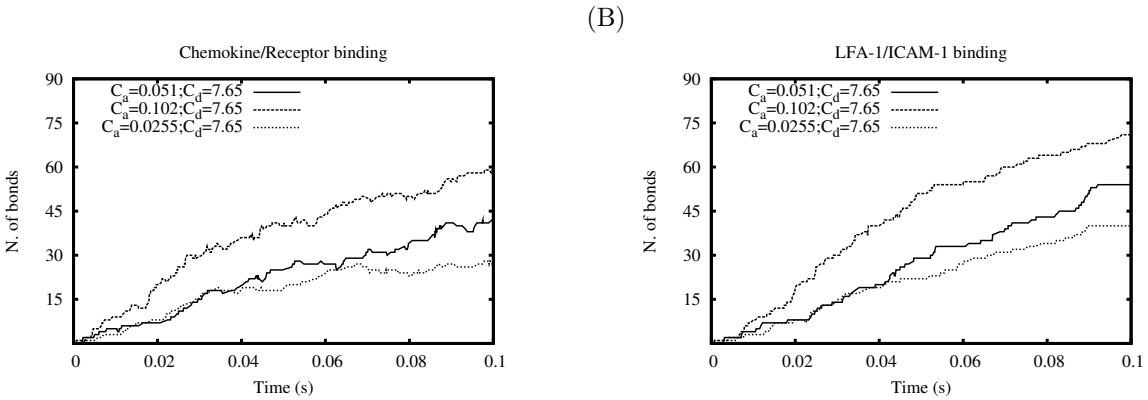

Figure 15: (A) The number of bonds between chemokines and their receptors at $C_d = 7.64$ but at $C_a = 0.051, 0.102, 0.0255$. (B) The LFA-1/ICAM-1 bindings that depends on the activation of chemokine's receptors.

The decrease in C_a to 0.0255 does not demonstrate the change in the amount of receptor/chemokine number of bonds and LFA-1/ICAM-1 binding. However, the increment in C_a from 0.051 (Fig.15, solid line) to 0.102 exhibits an apparent increase in the number of bonds both between chemokines and their receptors and LFA1 and ICAM1. It shows

that higher rate of dissociation only responds rapidly to appropriate association rate which lies above 0.051.

6 Conclusion

From the result we obtained, modification in the number of α_4-integrins and their receptors has no effect on the speed of binding reaction and on the rapidity of bnding between LFA-1 and ICAM-1 and thence ultimately on the rapidity of lymphocyte adhesion and diapedesis.

Different association and dissociation rate of chemotactic interactions reflects different levels of sensitivity. The work shows the high sensitivity of the time behavior of the number of bonds between LFA-1/ICAM-1 in response to the variations of rapidity of chemokine binding to its receptor. Generally, increasing the specific speed of chemokines reaction leads to a rapid activation of LFA-1, to an increased number of bonds of LFA-1 with ICAM-1, and thence to a more likely diapedesis, the phenomenon whose occurrence causes the typical disorders of autoimmune neurological diseases. The model is highly sensitive to variations of the chemockine complexation rate coefficient (C_a), and much less sensitive to variation of the dissociation constant (C_d). A brief summary of the third section of sensitivity analysis on the number of bonds of chemokines to their receptor and the number of bonds of LFA1/ICAM1 can be drawn, referring to the subsections of section 5.1.3 as in the following.

5.1.3.1 Given $C_a = 0.051$ and C_d= 3.81, the results from the 50% changes in C_d are approximately identical.

5.1.3.2 Given C_a=0.102, the model does not show differences from the cases in which C_d is between 1.91 and 7.65.

5.1.3.3 At a low C_a (≤ 0.025), the amount of bonds over the time is strongly relied on the dissociation rate and is positively correlated.

5.1.3.4 At rate C_d=3.82, the time course of the number of bonds between chemokine and its receptors and LFA1/ICAM1 is significantly affected when C_a is below 0.051.

5.1.3.5 The number of bonds LFA1/ICAM1 proportionally increases with C_a when $C_d = 1.91$.

5.1.3.6 Given C_d=7.64, the model will show significant difference when C_a is above 0.051.

References

[1] R. Alon, S. Chen, K. D. Puri, E. B. Finger and T. A. Springer, The kinetics of L-selectin tethers and the mechanics of selectin-mediated rolling, The Journal of Cell Biology, **138**(5), pp. 1169-1180, 1997.

[2] J. J. Campbell, J. Hedrick, a. Zlotnik, M. A. Siani, D. A. Thompson, E. C. Butcher. Chemokines and the arrest of lymphocytes rolling under flow conditions, Science, 279, 1998.

[3] K. Chang, D. F. J. Tees and D.A. Hammer, The state diagram for cell adhesion under flow: leukocyte adhesion and rolling, PNAS **97**(21), pp. 11262-11267, 2000.

[4] J. Choi, D.R. Enis, K.P. Koh, S.L. Shiao, and J.S. Pober, T lymphocyte-endothelial cell interactions Annual review of immunology Vol.22: 683–709, 2003.

[5] D. D'Ambrosio, P. Lecca, C. Priami, and C. Laudanna, Concurrency in leukocyte recruitment, Trends in Immunology, 25(8): 411-416, 2004.

[6] P. Degano and D. Prandi and C. Priami and P. Quaglia, Beta binders for biological quantitative experiments, ENTCS, 2005.

[7] L. Dematté, C. Priami, A. Romanel, BetaWB: modelling and simulating biological processes, In Procs of 2007 Summer Simulation Multiconference, pp. 777-784, 2007.

[8] E. Evans, A. Leung, D. hammer and S. Simon, Chemically distinct transition states govern rapid dissociation of single L-selectin bonds under force, PNAS **98**(7), 2001.

[9] J. Fritz, A. K. Katopodis, F. Kolbinger and D. Anselmettim Force-mediated kinetics of single P-selectin/ligand complexes observed by atomic force microscopy, PNAS **95** pp. 12283-12288, 1998.

[10] D. T. Gillespie, Exact stochastic simulation of coupled chemical reactions, The J. of Physical Chemistry, 81(25), 1977.

[11] M. R. King and D. A. Hammer, Multiparticle adhesive dynamics: hydrodynamic recruitment of rolling leukocytes, PNAS, **98**(26), pp. 14919-14924, 2001.

[12] M. R. King and D. A. Hammer, Hydrodynamic recruitment of rolling leukocytes: simulation and cell-free experiments, BED **50**, Bioengineering Confenrece ASME 2001.

[13] C. Laudanna, J. Y. Kim, G. Constantin, E. Butcher, Rapid leukocyte integrin activation by chemokines. Immunol. Rev. 186: 37-46, 2002

[14] P. Lecca, C. Priami,P. Quaglia, B. Rossi, C. Laudanna, G. Constantin A Stochastic Process Algebra Approach to Simulation of Autoreactive Lymphocyte Recruitment. SIMULATION Vol.80, No.6 273–288, 2004

[15] B. Marshall, R. P. McEver and C. Zhu, Kinetic rates and theri force dependence of the P-Selectin/PSGL-1 interaction measured by atomic force microscopy, BED **50** Bioengineering Conference ASME, 2001.

[16] R. Milner, Communicating and mobile systems: the π-calculus, Cambridge University Press, 1999

[17] L. Piccio, B. Rossi, E. Scarpini, C. Laudanna, C. Giagulli, A. C. Issekutz, D. Vestweber, D. C. Butcher, G. Constantin, Molecular mechanisms involved in lymphocyte recruitment in inflamed brain microvessels: critical roles for P-selectin glycoprotein ligand-1 and heterotrimeric G(i)-linked receptors. J Immunol 168: 1940–1949, 2002

[18] C. Priami and P. Quaglia, Beta binders for biological interactions, In Procs of CMSB 2004.

[19] A. Romanel, L. Dematte and C. Priami, The Beta Workbench, The Microsoft Research - University of Trento Centre for Computational and System Biology (available at http://www.cosbi.eu), TR 03, 2007

[20] D. W. Schmidtke and S. L. Diamond, Direct observation of membrane tethers formed during neutrophil attachment to platelets or P-selectin under physiological flow, The Journal of Cell Biology **149**(3), 2000.

[21] C. Zhu, G. Bao and N. Wang, Cell mechanics: mechanical response, cell adhesion and molecular deformation, Annu. rev. Biomed. Eng. **2**, pp- 189-226, 2000.

Appendix B: Lymphocyte's structure

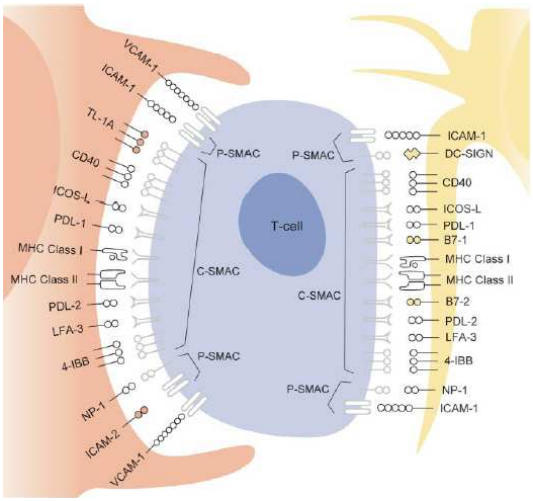

Figure 16: Comparison of EC and DC T cell contact regions. On the left side, this figure illustrates some of the membrane-bound molecules on the EC surface that may participate in antigen presentation and subsequent T cell activation. Depicted is a docking structure, unique to T cell/EC adhesion, that forms a membrane cup around the base of the T cell. Preliminary data suggest that, in the presence of antigen, an immune synapse can form within the docking structure, differentiating into a central supramolecular activation complex (c-SMAC), consisting of MHC and costimulatory molecules, and a peripheral supramolecular activation complex (p-SMAC), consisting of adhesion molecules. Such immune synapses are well formed in contacts between a T cell and classical antigen presenting cell (DC), which is shown on the right side of the figure. The molecules that are thought to be unique to either APC type are colored differentially, EC in pink and DC in yellow [4].

Appendix C: Configurations

Rate constants	Figure	Configuration
Original	8: solid line	$C_{assoc} = 2k_{on}/V \times 10^4$ $C_{dissoc} = k_{off}/V \times 10^4$
Rates decrease by 10^1	8: dashed line	$C_{assoc} = 2k_{on}/V \times 10^3$ $C_{dissoc} = k_{off}/V \times 10^3$
Rates decreased by 10^2	8: dotted line	$C_{assoc} = 2k_{on}/V \times 10^2$ $C_{dissoc} = k_{off}/V \times 10^2$
Different amount of VCAM-1		$C_{assoc} = 2k_{on}/V \times 10^4$ $C_{dissoc} = k_{off}/V \times 10^4$
	9: solid line	VCAM-1 = 15
	9: dotted line	VCAM-1 = 88
	9: dashed line	VCAM-1 = 176
Different C_a,C_d		Original amount of substances except VCAM-1=88
	10: solid line	$C_a = 0.051$, $C_d = 3.82$
	10: dashed line	$C_a = 0.051$, $C_d = 1.91$
	10: dotted line	$C_a = 0.051$, $C_d = 7.65$
	11: solid line	$C_a = 0.102$, $C_d = 3.82$
	11: dashed line	$C_a = 0.102$, $C_d = 1.91$
	11: dotted line	$C_a = 0.102$, $C_d = 7.65$
	12: solid line	$C_a = 0.0255$, $C_d = 3.82$
	12: dashed line	$C_a = 0.0255$, $C_d = 1.91$
	12: dotted line	$C_a = 0.0255$, $C_d = 7.65$
	13: solid line	$C_a = 0.051$, $C_d = 3.82$
	13: dashed line	$C_a = 0.102$, $C_d = 3.82$
	13: dotted line	$C_a = 0.0255$, $C_d = 3.82$
	14: solid line	$C_a = 0.051$, $C_d = 1.91$
	14: dashed line	$C_a = 0.102$, $C_d = 1.91$
	14: dotted line	$C_a = 0.0255$, $C_d = 1.91$
	15: solid line	$C_a = 0.051$, $C_d = 7.65$
	15: dashed line	$C_a = 0.102$, $C_d = 7.65$
	15: dotted line	$C_a = 0.0255$, $C_d = 7.65$

Table 3: The configurations of all simulations. The original settings in term of the amount are: Lymphocyte = 88 ; PSelectin = 88; ICAM = 86; VCAM = 15; Chemokine = 236. If there is no special remark, the configuration in amount is based on the original one.